The role of chemistry in the oscillating combustion of hydrocarbons: An experimental and theoretical study

A. Stagni, Y. Song, L A Vandewalle, K M van Geem, G B Marin, Olivier Herbinet, Frederique Battin-Leclerc, T. Faravelli

The role of chemistry in the oscillating combustion of hydrocarbons: An experimental and theoretical study

A. Stagni[a], Y. Song[b], L.A. Vandewalle[c], K.M. Van Geem[c], G.B. Marin[c], O. Herbinet[b], F. Battin-Leclerc[b], T. Faravelli[a]

[a]Department of Chemistry, Materials, and Chemical Engineering "G. Natta", Politecnico di Milano, Piazza Leonardo da Vinci 32, 20133 Milano, Italy
[b]Laboratoire Réactions et Génie des Procédés, CNRS-Université de Lorraine, 1 Rue Grandville, 54000 Nancy, France
[c]Laboratory for Chemical Technology, Ghent University, Technologiepark 125, Ghent B-9052, Belgium

Published in Chemical Engineering Journal 385 (2020) 123401
(https://doi.org/10.1016/j.cej.2019.123401)

Highlights

- Measurement of species mole fractions during oscillating combustion was performed.
- The establishment of limit cycles is observed also in quasi-isothermal conditions.
- 5 main recombination channels were found behind the oscillating behavior.
- Multiple unstable regions are established because of thermokinetic interactions.

Abstract

The stable operation of low-temperature combustion processes is an open challenge, due to the presence of undesired deviations from steady-state conditions: among them, oscillatory behaviors have been raising significant interest. In this work, the establishment of limit cycles during the combustion of hydrocarbons in a well-stirred reactor was analyzed to investigate the role of chemistry in such phenomena. An experimental investigation of methane oxidation in dilute conditions was carried out, thus creating quasi-isothermal conditions and decoupling kinetic effects from thermal ones. The transient evolution of the mole fractions of the major species was obtained for different dilution levels ($0.0025 \leq X_{CH_4} \leq 0.025$), inlet temperatures (1080 K$\leq T \leq$1190 K) and equivalence ratios ($0.75 \leq \varphi \leq 1$). Rate of production analysis and sensitivity analysis on a fundamental kinetic model allowed to identify the role of the dominating recombination reactions, first driving ignition, then causing extinction.

A bifurcation analysis provided further insight in the major role of these reactions for the reactor stability. One-parameter continuation allowed to identify a temperature range where a single, unstable solution exists, and where oscillations were actually observed. Multiple unstable states were identified below the upper branch, where the stable (cold) solution is preferred. The role of recombination reactions in determining the width of the unstable region could be captured, and bifurcation analysis showed that, by decreasing their strength, the unstable range was progressively reduced, up to the full disappearance of oscillations. This affected also the oxidation of heavier hydrocarbons, like ethylene. Finally, less dilute conditions were analyzed using propane as fuel: the coupling with heat exchange resulted in multiple Hopf Bifurcations, with the consequent formation of intermediate, stable regions within the instability range in agreement with the experimental observations.

Keywords: Low-temperature combustion; Oscillations; Bifurcation; Reactor stability; Methane

Nomenclature

Roman Symbols

P	Pressure [Pa]
T	Temperature [K]
X	Mole fraction [–]

Acronyms

CSTR	Continuous-Stirred Tank Reactor
DRGEP	Directed Relation Graph with Error Propagation
HB	Hopf Bifurcation
JSR	Jet-Stirred Reactor
LP	Limit Point
NOx	Nitrogen Oxides
PAH	Polycyclic Aromatic Hydrocarbons

Greek Symbols

α	Multiplier of reaction rates [–]
φ	Equivalence ratio [–]
τ	Residence time [s]

1. Introduction

Low-temperature combustion techniques allow to obtain a substantial decrease in the emission of pollutants like Nitrogen Oxides (NOx), Polycyclic Aromatic Hydrocarbons (PAH) and soot. Since they are also increasingly regulated [1], research efforts on such techniques have progressively increased in the last two decades. To achieve combustion at lower temperatures while simultaneously pursuing high thermal efficiencies, a number of novel combustion concepts has been developed, for both next-generation engines [2-4] and furnaces [5,6]. Regardless of the specific technology and of the involved fuels, chemistry plays a central role in such applications, since the assumption of infinitely fast reaction is no longer valid at lower temperatures. As a result, chemical kinetics may control the combustion process as a whole, and the operational stability of such processes is often not obvious.

From a modeling point of view, a comprehensive understanding of the underlying phenomena requires two main challenges to be addressed: (i) a thorough description of the complex chemistry in all its elementary steps is needed, and the use of detailed kinetic models for combustion is then imperative [7]; (ii) the possible deviations from a steady-state operation need a proper framing and characterization. In this regard, cool flames [8], multiple solutions [9,10] and oscillatory states [11] have often been observed. Specifically, the topic of oscillating modes in combustion has found significant attention within the scientific community. They are an important benchmark for the validation of kinetic mechanisms, since they involve thermochemical competitions due to the interaction between mass flow, heat exchange and chemistry resulting in a periodic extinction and reignition. The fundamental understanding of oscillations provides practical outcomes. As an example, it can be leveraged to ignite chemical reactors in a controlled way so the operating point can be stable on the ignited branch, which is already being used for example for oxidative coupling of methane [12,13]. Moreover, in several applications, such as burners, oscillations, which are undesired because of control issues, can occur in recirculation zones. Being able to model and predict these phenomena then allows to limit this behaviour.

The establishment of permanent oscillations has been observed in the oxidation of the smallest hydrocarbons in non-isothermal, well-stirred reactors for several decades [14]. The earliest studies on this topic were performed on the simplest fuels, i.e. hydrogen and syngas [15-22]: in such cases, the relative simplicity of the chemistry even allowed to carry out analytical studies. In the case of hydrogen [23], the mass balance of the H radical allowed a reasonably accurate prediction of the ignition temperature, as a function of pressure and inflow properties; an analytic expression of the oscillation frequency could be formulated [24]. It was shown that the periodic behavior was the result of the competition between branching and third-body reactions of the H radical with O_2. The rate of the latter significantly increases after ignition because of the third-body efficiency of water [25], causing extinction.

Simplified treatments are not possible when higher hydrocarbons are involved, because of the added chemical complexity. Oscillating limit cycles have been experimentally observed in the combustion of methane [11,26-31] as well as in ethane [32] and propane [33,34] at atmospheric pressures and temperatures around 1000 K. In the case of smaller hydrocarbons, a comprehensive explanation of such behavior has not been provided so far. The state-of-the-art studies of De Joannon, Sabia and coworkers [11,26-28,35] focused on methane oxidation at atmospheric pressure, and characterized the operating conditions where oscillations occur, by varying inlet temperature and equivalence ratio. Here, they observed different shapes in terms of temperature profiles in the explored regions, and verified that several kinetic models were able to predict such trends. The authors also hypothesized that CH_3 recombination reactions have a major role in causing oscillations as they subtract active radicals from the oxidation channel, and explained the establishment of oscillations as the result of the interaction between methane chemistry and heat loss in the surroundings. A major issue in investigating oscillating combustion in stirred reactors is the practical difficulty of decoupling kinetic aspects from thermal ones: periodic ignition and extinction give rise to significant temperature peaks, and the observed oscillations result from the interplay between chemistry, heat release and heat loss. From a modeling standpoint, Lubrano Lavadera et al. [29] performed isothermal simulations of methane oxidation for conditions under which oscillations were experimentally observed: periodic variations of species composition were still present, thus suggesting that the origin of oscillations is actually due to chemistry, as in the case of hydrogen [15,20]. By analyzing the different reaction rates in the transition from low temperatures to the onset of oscillations, they observed that oscillations occur when the rate of the branching reaction overcomes that of decomposition reaction of the hydrogen peroxide, hence causing ignition, whereas the recombination of CH_3 radicals inhibits the oxidation pathway. Moreover, they showed that, beyond the upper limit of the oscillations range, the rate of CH_3 recombination reaction with OH prevails over the self-recombination of CH_3, thus stopping the inhibition channel. Therefore, they concluded that the dynamic behavior finds its origin in kinetics, and is related to the competition between oxidation and recombination reactions involving carbon species as well as hydrogen.

This work aims at elucidating the role of chemical kinetics in the onset of oscillations during the combustion of small hydrocarbons in well-stirred systems. With the ultimate goal of providing a comprehensive understanding of the phenomena triggering this dynamic behavior, the issue is tackled through a threefold approach:

1. An experimental campaign in a Jet-Stirred Reactor (JSR) is performed under very diluted conditions, in order to limit thermal interactions. The time-varying mole fractions of the key species are also measured for the first time in this kind of systems.
2. A detailed kinetic model, describing the oxidation of hydrocarbons up to C_3, is used to interpret the experimental results and investigate the controlling mechanisms.
3. The transition from the low-temperature steady state to the oscillating region, and subsequently to the high-temperature steady state is analyzed by a bifurcation analysis. The stability of the system is investigated, with an emphasis on the way this is affected by the kinetic parameters.

2. Materials and methods

2.1. Experimental setup

Experiments were carried out in a fused silica Jet-Stirred Reactor (JSR), a type of Continuous Stirred Tank Reactor (CSTR) which is usually operated at steady state (unlike the present study). Such device has been used for a long time for gas-phase pyrolysis and oxidation kinetic studies [36,37], and only its main features are reported here. The JSR was designed to obtain a homogeneous composition and temperature in the gas

phase [38,39]: the homogeneity of the composition was previously verified through different criteria [40]. The system consists of a spherical reactor with four nozzles (inner diameter of 0.3 mm) at its center providing turbulent jets for the gas-phase mixing. Prior to flowing through the nozzles, the fresh gas mixture is progressively heated up to the reaction temperature to avoid temperature gradients in the gas phase. Both preheater and reactor are heated with Thermocoax resistances, and the heating is controlled through K-type thermocouples located between the resistances and the reactor wall. The reaction temperature is measured with an independent K-type thermocouple located in a glass finger, the extremity of which is close to the center of the reactor (the maximum uncertainty in the temperature measurement is ±5 K). Fresh gas flow rates are controlled with mass flow controllers provided by Bronkhorst (the relative uncertainty in flow rates is ±0.5%, which leads to a relative uncertainty of ± 1% on the residence time and on the equivalence ratio).

As opposed to previous kinetic studies [36-39], the present work requires the measurement of the species mole fractions in the JSR as a function of the time. A specific analytical method was developed for this purpose, based on two major principles: (i) the direct sampling of the gas phase in the jet-stirred reactor, and (ii) a fast sampling analysis. To achieve this goal, a mass spectrometer with online sampling using a capillary tube was used. This apparatus was provided by Pfeiffer Vacuum (Omnistar model). The sampling line was made with a stainless steel capillary tube (2 meter long, inner diameter of 0.120 mm and heated to 423.15 K) which was extended by a fused silica capillary tube (0.5 meter long, inner diameter of 0.100 mm and at ambient temperature). The fused silica part was connected to the reactor, whereas the stainless steel part was connected to a quadrupole mass spectrometer (mass range: 1–200 amu, resolution: 0.5–2.5, ionization by electronic impact at 70 eV). The quadrupole scan time was about 360 ms, which allowed about 3 measurement points per second. This sampling rate was fully compatible with the observed period of oscillations. Note that radical species cannot be detected using this technique, as they recombine in the transfer line between the reactor and the mass spectrometer.

The time evolution of species concentrations was followed based on characteristic m/z ratios (e.g., m/z 16 for methane). Raw signals recorded for m/z 16, 18, 28, 30, 32 and 44 are displayed in the Supplementary Material (Figure S1). A particular attention was paid to the calibration of the analytical device. Standards were required for each individual species as they all behave differently as far as ionization and fragmentation are concerned. Calibration curves were obtained by measuring signals for mixtures of pure standards (methane, oxygen, or carbon dioxide) diluted into helium using mass flow controllers. Calibration curves for CH_4, O_2 and CO_2 are displayed in Figure S2 in supplementary material. Water (m/z 18) was not calibrated.

Ions formed during the ionization process have an energy excess (ionization at 70 eV) and tend to fragment into smaller ions and neutral species. In the present work, the studied system is rather simple, i.e., when oscillations occur the reaction products are mainly water and carbon dioxide. Therefore, no evidence of large interferences due to ion fragmentation was observed for the m/z of interest. However, to obtain more accurate methane mole fractions, the signal obtained for m/z 16 was systematically corrected to account for the contribution of the fragments coming from O_2^+ and CO_2^+. These contributions were deduced from the calibration of pure standards (see Figure S2 in supplementary material). The fragmentation of water, which was not quantified, could also contribute to the signal at m/z 16, but the abundance of the O^+ fragment was low according to the water mass spectrum from the NIST database [41]. A similar observation could be done for the contribution of CO to the signal at m/z 16.

The carbon balance was calculated for each experiment. It is in the range 81–118% with standard deviations in the range ± 4–9% (see Table S1 in supplementary material). This could be due to uncertainties

in the measurement (sampling) and in the calibration, and also due to the absence of mole fraction measurements of carbon containing species like CO (m/z 28 in the graphs of Figure S1).

2.2. Kinetic model and validation

The kinetic mechanism used to simulate the experimental results, and consequently investigating the mechanisms triggering oscillations, was obtained from the CRECK kinetic framework. Such framework describes the pyrolysis, partial oxidation and combustion of hydrocarbon fuels up to C_{16}. In particular, the methane mechanism was originally developed by Ranzi et al. [42], and was initially made up of 78 species and ~1600 reactions. This was constructed using an approach based on 5 reaction classes, while adopting similarity and analogy rules [43] to automatically estimate the kinetic parameters of H-abstraction reactions; general rules were also used for isomerization reactions of larger radicals. The performance of the obtained mechanism was successfully verified in a wide range of operating conditions: in addition to the pyrolysis, autoignition and combustion of methane, the oxidation of methanol and formaldehyde, as well as the pyrolysis and oxidation of C_2 species (e.g. ethane, ethylene, acetaldehyde) were successfully benchmarked. Recently, the core C_0-C_3 mechanism was revised by implementing the H_2/O_2 and C_1/C_2 subsets proposed by Metcalfe et al. [44] and C_3 from Burke et al. [45]. Thermodynamic properties were updated, too, using the database of Burcat and Ruscic [46]. The resulting mechanism includes 115 species and 1852 reactions. A comprehensive validation of the methane mechanism is available in previous works [29-31].

In order to ease the computational load of the theoretical analysis, a conservative skeletal reduction was applied to the kinetic mechanism. To this purpose, the multi-step methodology illustrated in [47] and implemented in the DoctorSMOKE++ software was utilized. In this methodology, the Directed Relation Graph with Error Propagation (DRGEP) [48] is combined with a sensitivity analysis on species [49], with the target of a maximum error of 10% on ignition delay time. The operating conditions used for reduction are listed in Table 1.

Table 1. Operating conditions used for the reduction of the methane kinetic mechanism.

	Min	Max
Temperature	800 K	1800 K
Pressure	1 atm	
Equivalence ratio	0.5	2
CH_4 mole fraction	0.0025	0.05

The obtained skeletal mechanism is made up of 34 species and 349 reactions, and is available as Supplemental Material of this work. Figure 1 shows the capability of the skeletal mechanism in predicting the laminar flame speed of methane at different inlet temperatures, which is typically considered as an important benchmark for kinetic mechanisms [51]. Results are quite satisfactory, also considering the experimental uncertainty. The validation was completed through the prediction of species formation in ideal reactors. Sample results are shown in Figure 2, for the lean oxidation of methane experimentally investigated by Le Cong et al. [52]. A good agreement with the measurements is again observed, both for major species and intermediates, thus supporting the use of the skeletal mechanism for the prediction of the speciation in the oscillating system. Further validation of the methane mechanism in stirred reactors is available in previous works [29-31].

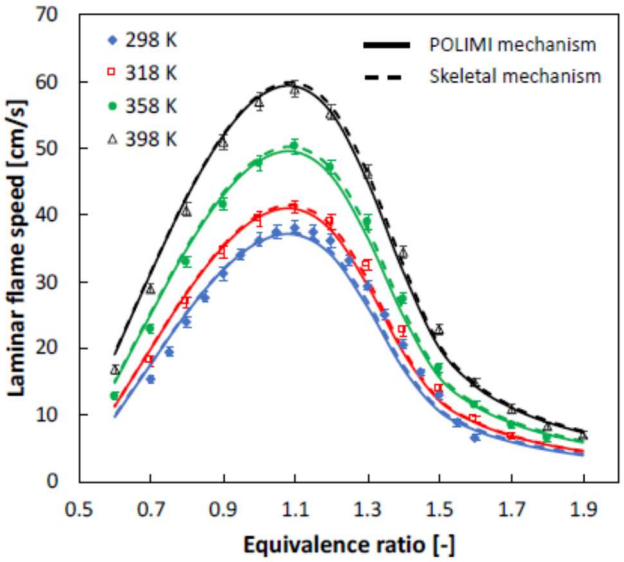

Figure 1. Experimental measurements [50] and modeling predictions of laminar flame speed of methane in air, at atmospheric pressure.

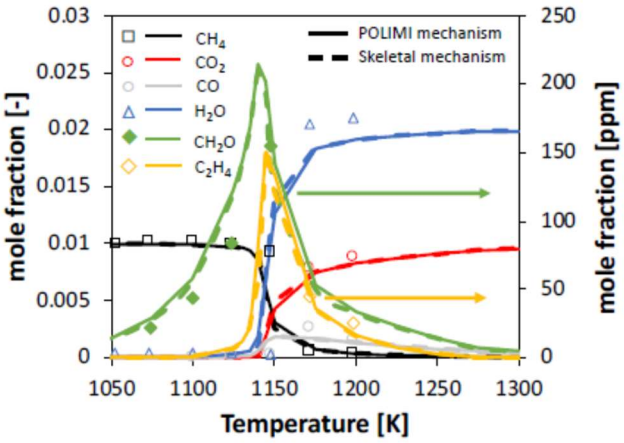

Figure 2. Experimental measurements [52] and modeling predictions of species formation in methane combustion in a JSR. P = 1 atm, τ = 0.12 s, φ = 0.3, X_{CH_4} = 0.01.

2.3. Bifurcation theory and tools

A theoretical understanding of the oscillatory behavior can be obtained via bifurcation analysis. This has been proven to be a very powerful tool in chemical engineering, mainly for identifying periodic behavior, reactor instabilities, multiplicity of steady states and their dependence on the chosen operating conditions [53-56]. Such analyses are mostly performed using simplified reactor models and a small amount of species, in order to limit the number of variables [57]. Kalamatianos and Vlachos [58] studied ignition, extinction and oscillations in a CSTR for hydrogen combustion, using a kinetic mechanism consisting of 20 reactions between 9 species. Even with their lumped parameter system, a complex bifurcation behavior was observed, in which the existence of either subcritical or supercritical Hopf Bifurcations (HB) [23] causes oscillatory ignition and multiple oscillatory extinction points. As detailed kinetic mechanisms are more suitable for extrapolation, their usage in bifurcation analyses leads to more accurate results, at the cost of higher computational demands and numerical instabilities [57]. In the last decade, remarkable progress has been made, mainly supported by the integration of detailed kinetic mechanism interpreters in bifurcation analysis codes [13,59-61]. One of the most comprehensive studies so far is the one by

Kooshkbaghy et al. [61], who studied the dynamics of n-heptane/air mixtures in CSTRs using a skeletal mechanism with ~150 species. They were able to perform both one- and two-parameter continuations revealing oscillatory behavior, multiplicity, isolas and codimension-two bifurcations.

In the present work, a bifurcation analysis of an isothermal CSTR for oxyfuel combustion was performed using the continuation and bifurcation software package AUTO-07P [62], which is one of the most widely used open-source bifurcation analysis tools in multiple engineering and scientific application areas. A detailed description of the methodology can be found in the work of Vandewalle et al. [13]. AUTO-07P was coupled to Cantera [63] as mechanism interpreter and IdealGasReactor model was directly used to model the isothermal CSTR. Following the guidelines by Lengyel and West [57], a central-differencing algorithm was used to calculate the numerical Jacobian, using a separate relative step size for each variable. Furthermore, a logarithmic transformation of all variables was applied to deal with the problem of large variations in the orders of magnitude of the species mass fractions.

The skeletal mechanism described in the Section 2.2 was used for such bifurcation analysis. One-parameter bifurcation curves were constructed, with the reactor temperature as bifurcation parameter. The influence of the residence time τ, equivalence ratio φ, and dilution on the bifurcation behavior was investigated. Furthermore, by applying a multiplication factor to the reaction rates, the crucial reactions responsible for the oscillatory behavior were studied.

3. Results and discussion

3.1. Limit cycles: speciation and frequency

A reasonable capability of predicting the boundaries of the oscillating region for $CH_4/O_2/He$ mixtures was already observed by Lubrano Lavadera et al. [29] at relatively low dilution levels ($X_{CH_4} \geq 0.01$) and lean-to-stoichiometric equivalence ratios ($0.75 \leq \varphi \leq 1$). Following their findings, the dynamic behavior of the major species throughout oscillations was sampled in several characteristic points (Table 2) of the space belonging to the quasi-isothermal region.

Table 2. Experimental conditions investigated for frequency analysis and species sampling throughout oscillating limit cycles.

ID	X_{CH_4}	X_{O_2}	X_{He}	φ	T (K)	ΔT_{exp} (K)
1	0.025	0.05	0.925	1	1080	25
2	0.01	0.02	0.97	1	1110	12
3	0.01	0.02	0.97	1	1140	8
4	0.005	0.01	0.985	1	1135	3
5	0.005	0.01	0.985	1	1175	3
6	0.005	0.01	0.985	1	1190	3
7	0.0025	0.005	0.9925	1	1175	2
8	0.0025	0.005	0.9925	1	1180	2
9	0.0025	0.005	0.9925	1	1190	2
10	0.01	0.0267	0.9633	0.75	1075	10
11	0.01	0.0267	0.9633	0.75	1100	10
12	0.01	0.0267	0.9633	0.75	1125	7

Figure 3 shows the time evolution of the major species for some characteristic operating conditions. To obtain these figures, the experiments and the model predictions were first aligned in terms of the first ignition, thus omitting the initial transients. It can be observed that the experimental profiles are reasonably well reproduced by the numerical model. For all of the considered cases, the modeled shape of

the CH_4 and O_2 mole fraction evolution during the extinction phase is in agreement with the experimental findings, and the observed peaks are mostly within the experimental uncertainty: for O_2, the average error on the peak mole fraction is 12%, with only two test cases (1 and 10, respectively) outside the experimental uncertainty. It must also be noticed that the minimum mole fraction of both reactants measured during the cyclic ignition is significantly higher than zero, while simulations show a complete consumption of reactants, regardless of the operating conditions. This discrepancy can be attributed to the very steep gradient of the mole fraction evolution profiles during the ignition process, such that the sampling system is not able to fully resolve species consumption at this stage.

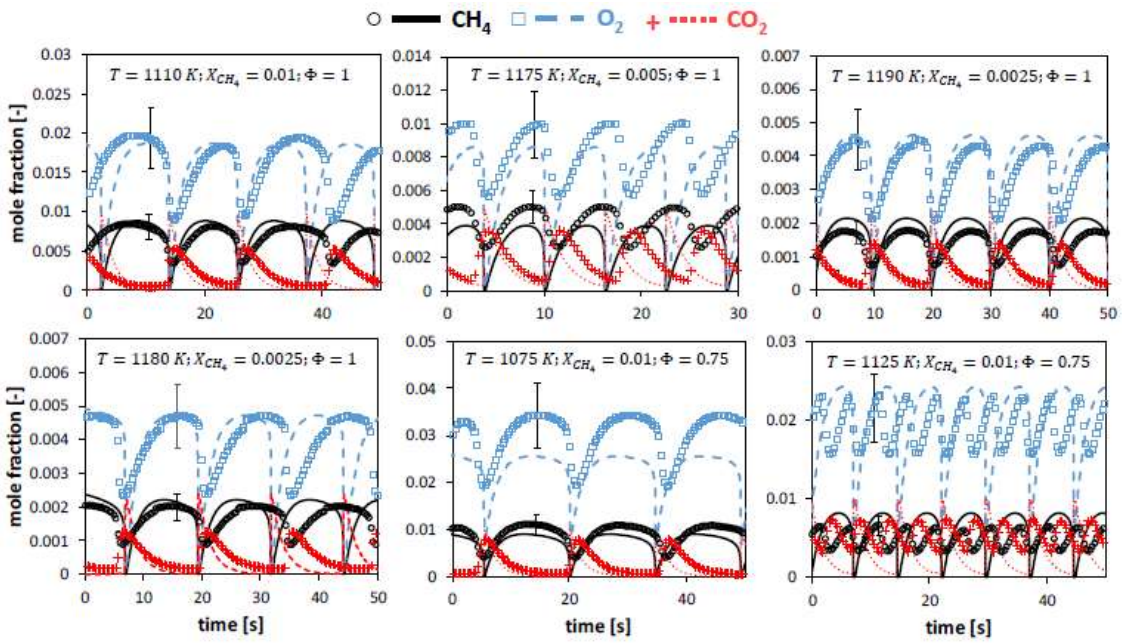

Figure 3. Time evolution of CH_4, O_2 and CO_2 mole fraction in the oscillating combustion of CH_4 in a JSR. Experimental data (symbols) vs kinetic modeling (lines) results (P = 107 kPa, τ = 2 s).

A frequency analysis is shown in Figure 4 for different operating conditions. The experimental uncertainty is hereby evaluated as the standard deviation of the measured oscillation frequency of the three major species. Taking this uncertainty into account, the agreement between experiments and numerical predictions is satisfactory: the average relative error in predicting frequency is ~14%, with a maximum deviation of ~36% for the test case 12. The model performs best in the most diluted conditions (i.e. X_{CH_4} = 0.25%), where thermal effects are less important. On the other side, the rate of frequency increase with temperature is underpredicted for X_{CH_4} = 1% in stoichiometric conditions, whereas good results are obtained in leaner conditions (φ = 0.75). As could be expected, both model results and experiments show an increase in frequency for a decrease in equivalence ratio at a constant inlet concentration of methane (1%), due to the higher oxygen concentration.

In order to frame the role of chemistry in the establishment of these limit cycles, a parametric analysis of the role of heat exchange in the JSR was carried out, such to identify the operating conditions for which chemistry can be sufficiently decoupled from heat release and heat loss phenomena. Indeed, once the reactor materials and geometries are defined (Section 2.1), the remaining variables governing thermal characteristics are the dilution level X_{CH_4} and the equivalence ratio φ.

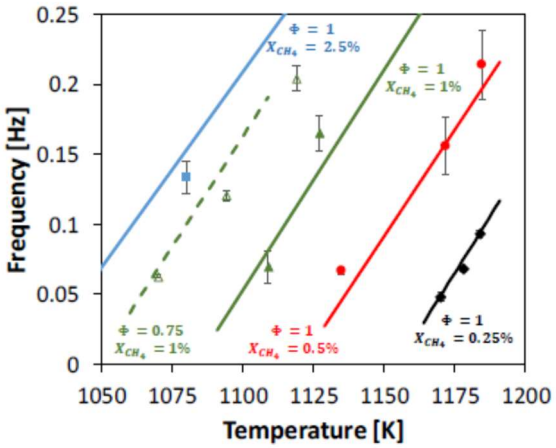

Figure 4. Observed vs predicted frequency of oscillations (in Hz) in several operating conditions. Experimental data (symbols) vs kinetic modeling (lines) results (P = 107 kPa, τ = 2 s).

Quasi-isothermal conditions were identified through a numerical analysis of the temperature increase following each ignition, and the effects of heat release were evaluated by comparing the oscillation frequencies and the width of the region characterized by oscillatory behavior. Figure 5 shows a parametric analysis of the oscillations frequency in stoichiometric conditions, obtained via spectral density estimation [64] with and without the hypothesis of isothermal operation. As observed in the earlier works [11,28-30, 35], oscillations are present between 1000 and 1250 K. The lower temperature limit of the oscillatory range is not sensitive to heat exchange, and virtually overlaps for the isothermal and non-isothermal case. On the other hand, the higher temperature limit increases in isothermal conditions, hence broadening the oscillatory operating range, especially for lower dilution levels. This is an expected behavior, since the heating of the mixture due to ignition increases the actual temperature inside the JSR in non-isothermal conditions, thus favoring an upper steady state. This effect is also strictly connected to the expected temperature oscillations in non-isothermal conditions, shown in Figure 6 for different equivalence ratios: in general terms, the amplitude of temperature oscillations varies from a few tens of K, in very diluted conditions, to several hundreds. Yet, as also previously noticed [29,30], such an increase is not observed experimentally, where in most of times the observed amplitudes are lower by an order of magnitude. As hypothesized in the previous work [29], this is most probably related to the steep dT/dt due to ignition, too fast to allow an accurate temperature resolution over time by the available thermocouple.

Figure 7 shows the thermal effects on the characteristics of limit cycles, as well as amplitude and frequency in sampled conditions. It can be observed that limit cycles of CH_4 vs O_2, CO_2 and HO_2 follow similar trajectories, with both isothermal and non-isothermal models, and are overlapped at the highest dilution rates. Because of the high dilution and very short ignition time scales, shorter than the duration of a single cycle, there are only small differences between the oscillation characteristics of the isothermal and non-isothermal case. In the investigated operating range, the difference in amplitude is negligible, whereas, in the worst case (Figure 7a), the maximum difference in the predicted frequency is ~25%. Above all, in most of the region where oscillations are predicted by both models (Figure 5), the difference in frequency is lower than 10%.

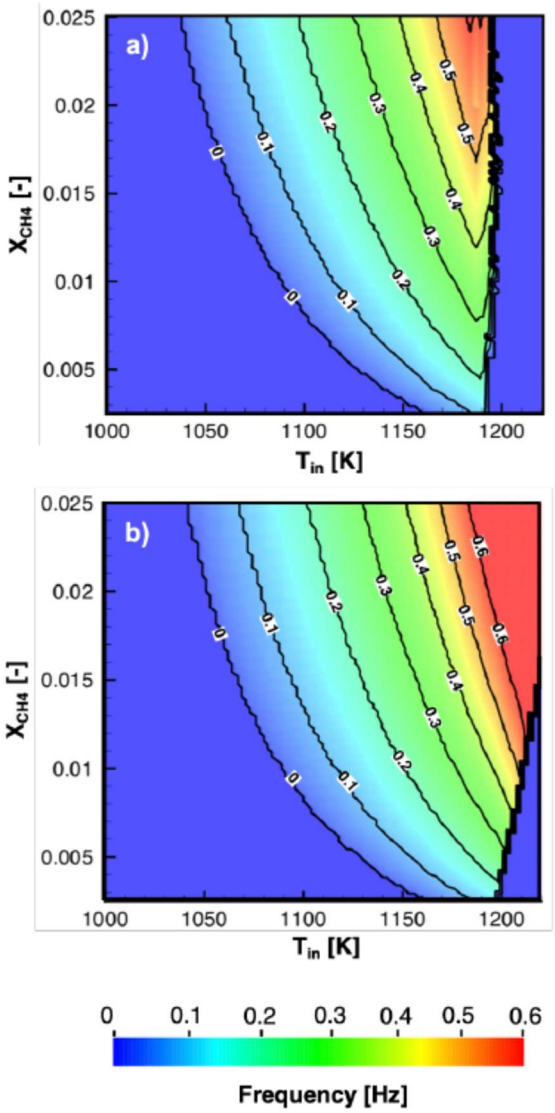

Figure 5. Predicted frequency of oscillations, as a function of inlet temperature and CH_4 dilution (φ = 1, P = 107 kPa, τ = 2 s): (a) Non-isothermal model. (b) Isothermal model.

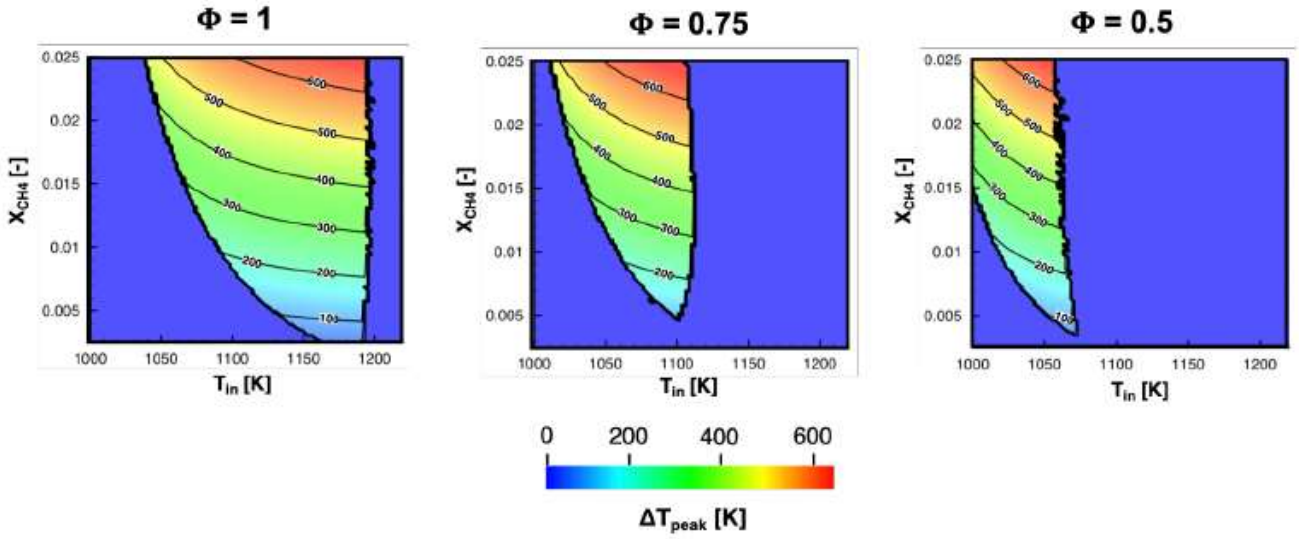

Figure 6. Predicted temperature increase due to ignition in the oscillating region, at different equivalence ratios (P = 107 kPa, τ = 2 s).

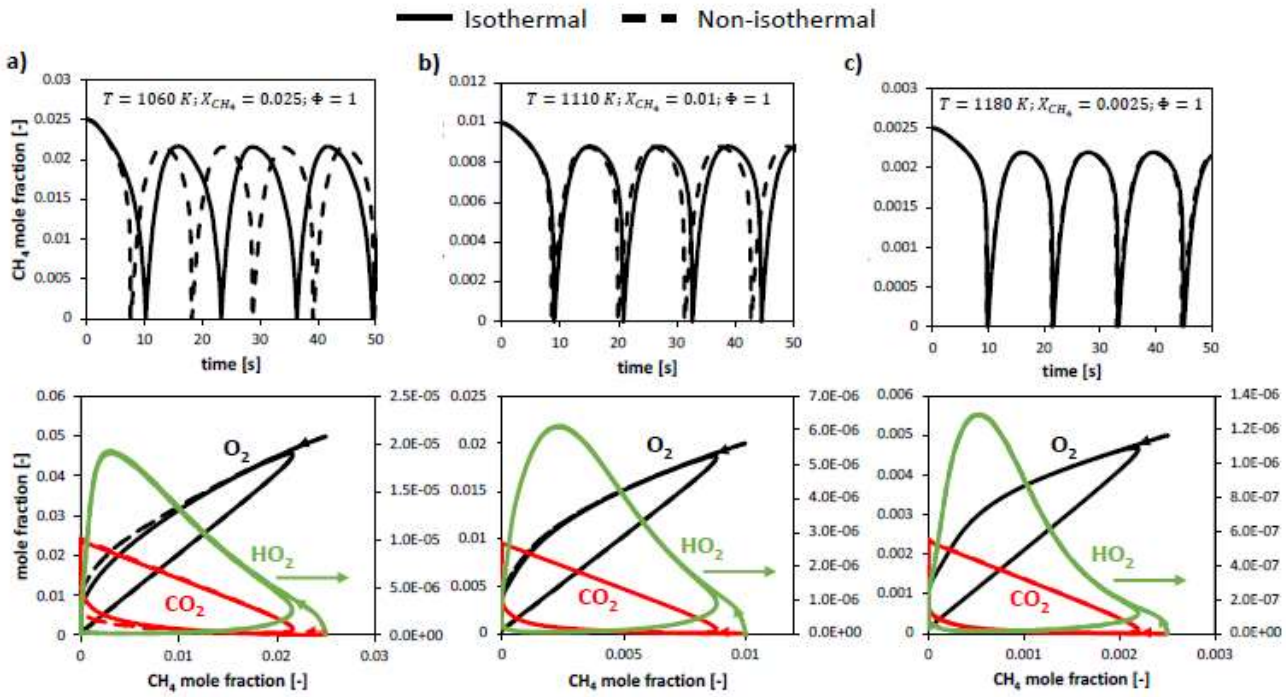

Figure 7. Comparison between time profiles of CH_4 (upper row) and limit cycles (lower row), as predicted with isothermal and non-isothermal models (P = 107 kPa, τ = 2 s).

In order to identify the critical, competing pathways resulting in temporal oscillations, the kinetic model was applied to investigate the evolution of the key species involved in the cyclic ignition and extinction. Figure 8 shows the time evolution of several key species in stoichiometric and lean conditions, respectively. In both cases, it can be observed that the build-up of radicals and consequent ignition follows that of a closed system with the same composition, although being slower because a part of such radicals is lost through the outflow. Afterwards, extinction follows and CH_3 concentration drops to zero, but the simultaneous inflow of CH_4 restarts the accumulation of methyl radical (and methyl-containing molecules, e.g. CH_3OH) in the system. After ignition, the decay rate of O, H and especially OH radicals is slower than that of CH_3 radical, thus allowing the continuation of H-abstraction reactions on CH_4. After such radicals are depleted, CH_3 decreases again and its further build-up is then controlled by the accumulation of methane. A clearer view of the transition between ignition and extinction, and the consequent onset of oscillations, is provided through the sensitivity analysis of the formation of OH (used as an indicator of reactivity) shown in Figure 9 for three characteristic times indicated in Figure 8. For both stoichiometric and lean conditions, a common trend can be observed before ignition: the branching reaction $H + O_2 \rightarrow OH + O$ has the highest inhibiting effect on reactivity. This peculiar effect had already been found by Bagheri et al. [30], and can be explained by the competition of such reaction with H-abstraction of H radical on CH_4, which instead promotes reactivity. On the other hand, the formation of C_2H_6 via methyl recombination enhances reactivity due to the higher reactivity of C_2H_6, if compared to CH_4. A similar effect is shown by the third-body reaction of H with O_2, which contributes to the accumulation of the HO_2 radical pool, needed for triggering ignition (cfr. Figure 8). After ignition, recombination reactions have an opposite effect: in stoichiometric conditions, terminations involving H radical (with CH_3, O_2 and, to a minor extent, OH) mostly cause the depletion of the radical pool. On the other hand, with a leaner mixture, extinction is controlled by oxygenated species, i.e. H recombination with O_2, and CH_3 recombination with OH forming CH_3OH. The establishment of oscillations is then determined by the re-accumulation of radicals following extinction: in this time range, it can be observed that terminations keep inhibiting reactivity. In stoichiometric conditions, CH_3 recombination to C_2H_6 subtracts active radicals from the system, thus preventing the establishment of a steady state, and completely estinguishing the system. In leaner conditions, the recombination to CH_3OH

has a twofold effect: on the one hand, it removes two active radicals from the pool, contributing to the complete extinction of the reactor; on the other hand, the higher concentration of CH_3OH interestingly results in a successive, light ignition (at t = 4.75 s), as confirmed by the second peak of OH present in Figure 8. Yet, the consequence of this second peak is the complete consumption of the active radicals (CH_3, H, OH, HO_2) and the consequent impossibility to reach a high-conversion steady state.

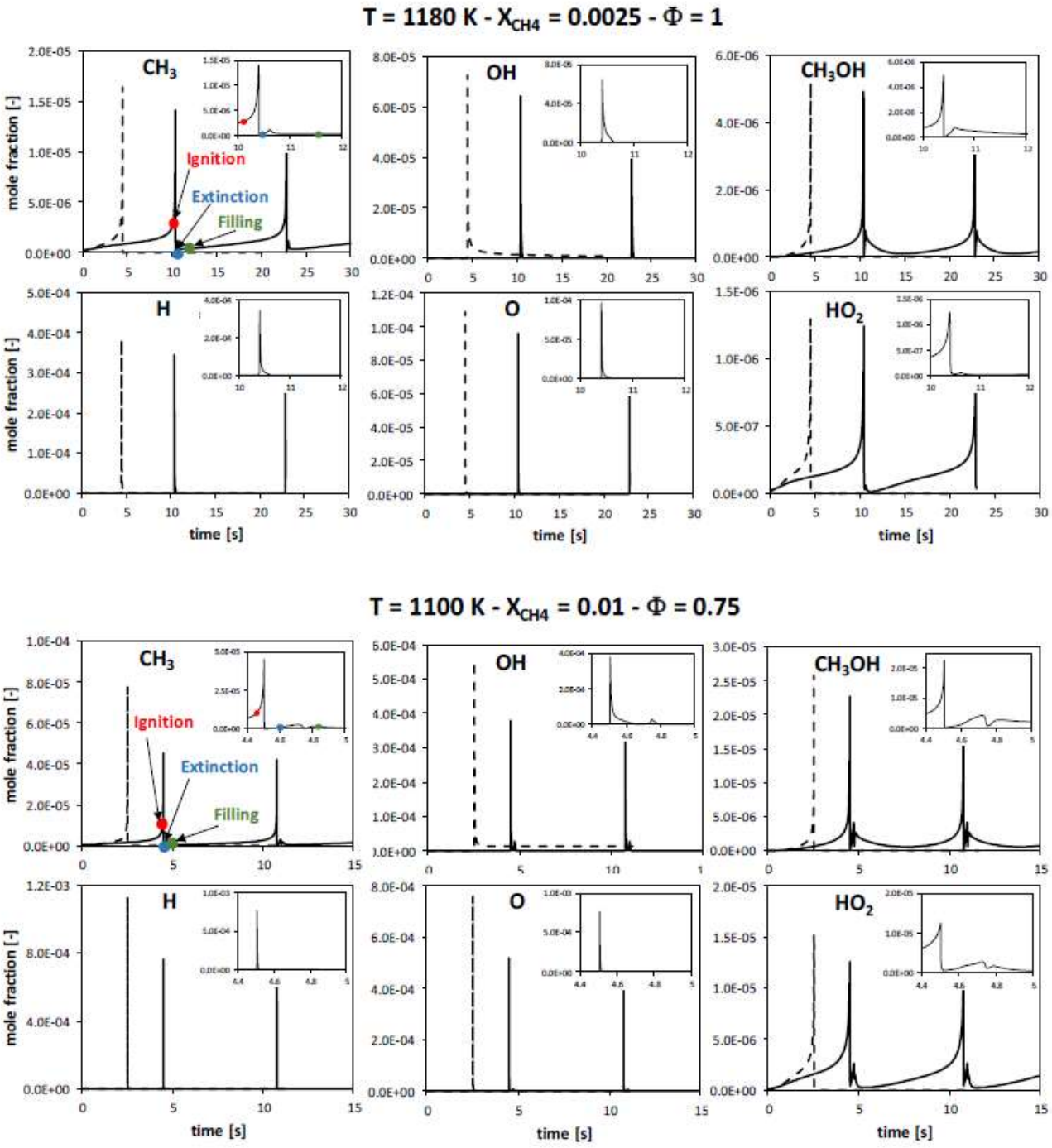

Figure 8. Continuous lines: predicted time profiles of key species in two representative conditions, with a close-up in the ignition/extinction region. Dashed lines: ignition in a batch reactor with the same initial composition (P = 107 kPa, τ = 2 s).

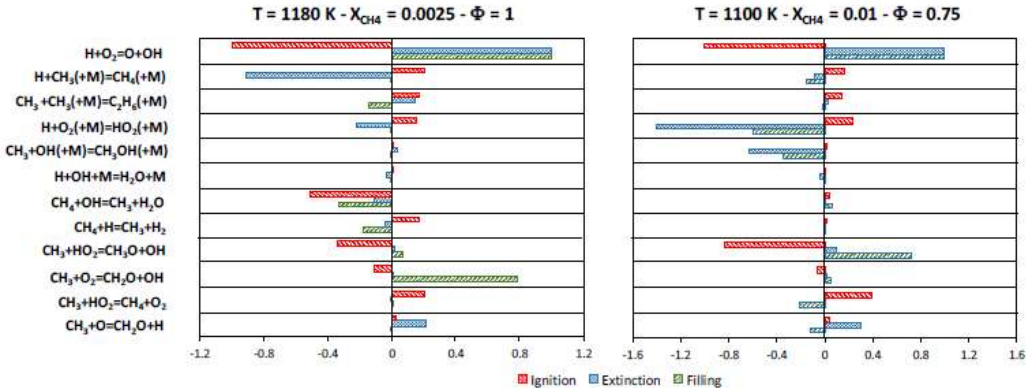

Figure 9. Sensitivity coefficients to OH formation in the three conditions indicated in Figure 8, normalized with respect to the sensitivity coefficient of $H + O_2 \rightarrow OH + O$.

3.2. Bifurcation analysis

Figure 10 shows CH4 mole fraction in an isothermal CSTR as a function of the operating temperature for a selected φ and X_{CH_4}. The full black line indicates a stable steady-state value, whereas the dashed line indicates an unstable or oscillatory steady state. The figure insets show the transient behavior of the methane mole fraction for 3 different operating temperatures. Multiplicity of steady states is observed between the two limit points (LP), i.e. the extinction point at 1049 K and the ignition point at 1086 K. A Hopf bifurcation (HB) exists at a temperature of 1208 K. The location of this HB with respect to the ignition and extinction points determines the stability of the system. This was similarly discussed by Kalamatianos and Vlachos in the case of H_2 oxidation [58], where it was also shown that the location of this HB varies with the operating conditions, i.e., P, τ and φ. Figure 10 is a typical example of a one-parameter continuation diagram with one HB outside the multiplicity region. By decreasing T on the ignited branch, oscillations start in proximity of the HB at 1208 K. Starting from the HB, this line extends to slightly higher temperatures, with the peak amplitude growing rapidly in the vicinity of 1210.7 K. It then folds back to lower temperatures, the peak amplitude still increasing. This hysteresis behavior, which indicates the subcritical nature of the HB, is not immediately observed in Figure 10a because of the narrow temperature window in which the phenomenon occurs. A close-up in proximity of the HB (Figure 10b) gives a clearer picture of the behavior. The hysteresis explains why oscillations can also be observed at temperatures slightly higher than the HB (i.e. between 1208 K and 1210.7 K). It is possible that an unstable branch, folding back at higher temperatures and creating a smoother transition between the low and high amplitude oscillations, exists as well. However, this was not detected with the adopted methods. With a decrease in temperature, oscillations are sustained until the ignition temperature is reached. Because the ignited state between the extinction temperature and HB is unstable, the system is driven to the stable non-ignited state through oscillations (oscillatory extinction). At lower temperatures, oscillations are no longer observed.

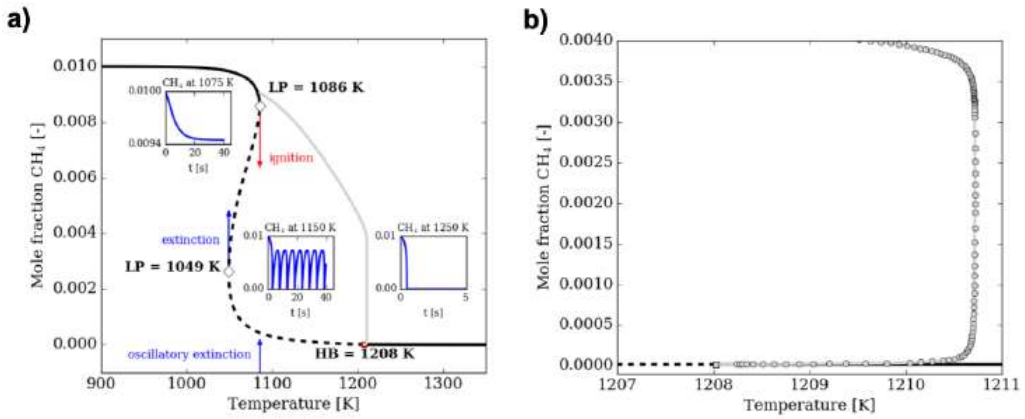

Figure 10. Steady-state CH_4 mole fraction in an isothermal CSTR as a function of the operating temperature. Gray line: peak CH_4 mole fraction during the corresponding oscillations. (a) Full temperature range (■: Hopf bifurcation, ◊: fold); (b) Close-up in proximity of the HB. φ = 1, X_{CH_4} = 0.01, P = 107 kPa, τ = 2 s.

The same type of continuation diagram can be constructed for different CH_4 dilution levels, and the data are shown in Figure 11. Oscillatory behavior can be expected in the dashed region between the ignition point and HB. These results are in good agreement with those presented earlier in Figure 6.

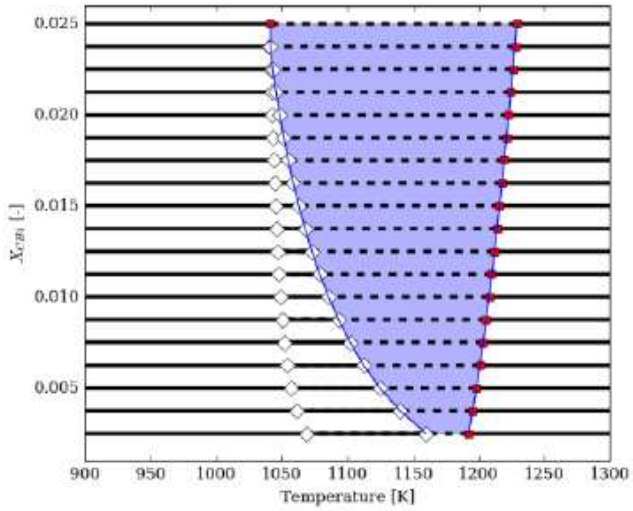

Figure 11. Map showing the effect of CH_4 dilution on the bifurcation behavior. Oscillations are observed in the blue region where a dashed line indicates the instability of the steady state. φ = 1, P = 107 kPa, τ = 2 s. (■: Hopf bifurcation, ◊: fold).

Gray and Scott [23] showed that chain branching (autocatalysis) is considered responsible for the steady state multiplicity, while termination reactions play a crucial role in the oscillatory behavior. The analysis of the phenomenology of oscillations carried out in Section 3.1 identified, for stoichiometric and lean conditions, five critical recombination steps in methane combustion, preventing the system from reaching a hot steady state. They are the following:

$H + CH_3(+M) \leftrightarrow CH_4(+M)$ (1)

$CH_3 + CH_3(+M) \leftrightarrow C_2H_6(+M)$ (2)

$H + O_2(+M) \leftrightarrow HO_2(+M)$ (3)

$CH_3 + OH(+M) \leftrightarrow CH_3OH(+M)$ (4)

$H + OH + M \leftrightarrow H_2O + M$ (5)

Their kinetic rates were taken from [65-69]. Figure 12 shows the bifurcation diagrams for the same lean and stoichiometric mixtures as previously shown in Figure 8. Temperature is used as bifurcation parameter, and the curves are constructed for different values of a multiplier α, applied to the rate of the controlling recombination pathways, as indicated by the sensitivity analysis (Figure 9). For the stoichiometric mixture, the progressive reduction of reactions (1), (2), and (3) has a clear influence on both the shape and the position of the curves. The ignition temperature, extinction temperature and Hopf bifurcations all shift to lower temperatures with a decreasing value of α. When the rate of these recombination reactions is reduced by a factor of 2 or more, HB occurs at a lower temperature than the ignition temperature. In this scenario, the system would be driven from the unstable ignited branch to the non-ignited branch, and sustained oscillations would not be observed. For the lean mixture, the application of α on the rates of reactions (1), (3), (4) has a limited influence on the ignition temperature, but causes a shift of the extinction temperature and HB to lower temperatures. With a decreasing rate of these recombination reactions, the region in which sustained oscillations are observed, would reduce and eventually vanish.

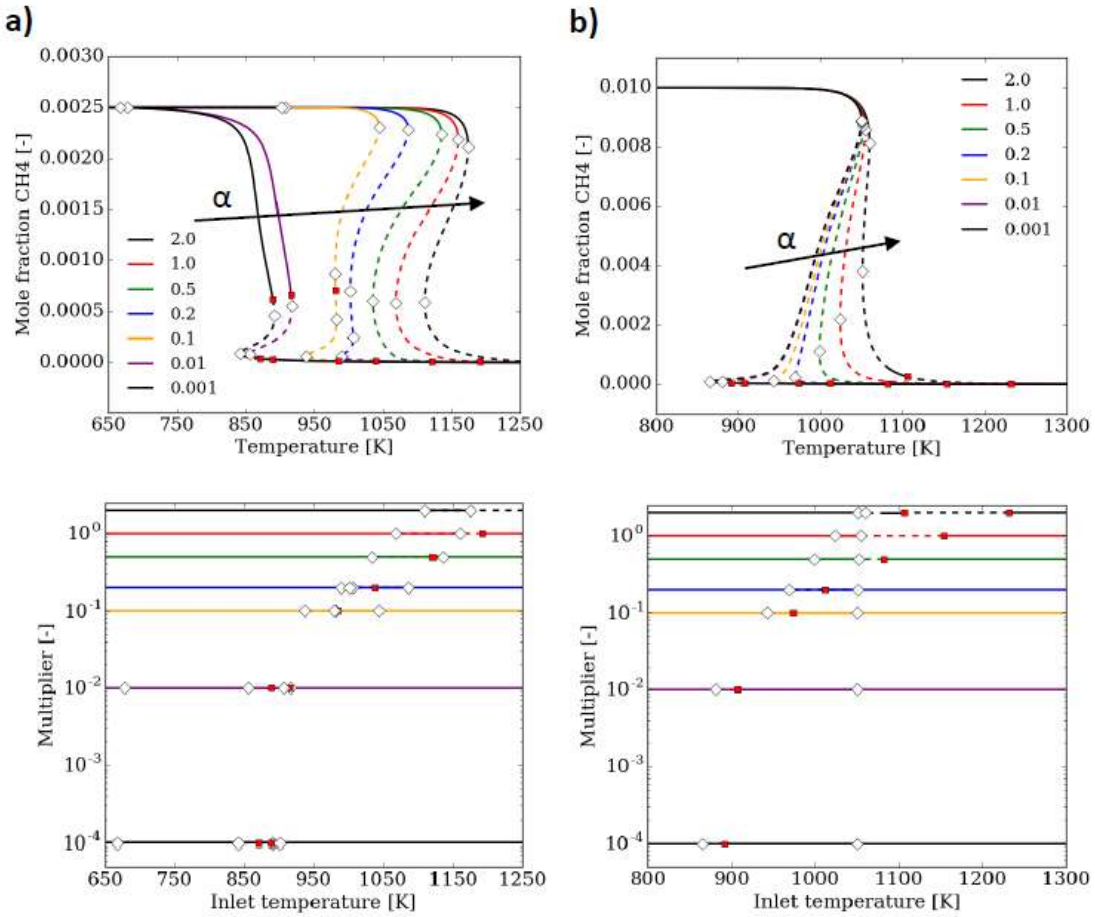

Figure 12. Influence of termination reactions on oscillation behavior. P = 107 kPa, τ = 2 s. (a) φ = 1, X_{CH_4} = 0.0025: α applied to reactions (1), (2), (3); (b) φ = 0.75, X_{CH_4} = 0.01: α applied to reactions (1), (3), (4). (■: Hopf bifurcation, ◊: fold)

It must be noted that termination step (3) was also identified by Tomlin et al. [21] as the main termination step throughout the hydrogen oxidation process. However, during the ignition phase, radical–radical termination reactions, such as reaction (5), were also found to be important. Tomlin et al. [21] concluded that the removal of these reactions would lead to changes in the oscillation period. This is in agreement

with the findings of this work, but for the conditions considered here, their removal would not be sufficient to ensure a complete disappearance of the oscillatory behaviour, since methyl chemistry must be considered, too.

3.3. Higher hydrocarbons: the case of ethylene

Due to the hierarchical nature of combustion mechanisms, the reactions (1)–(5) analyzed in Section 3.2 are also involved in the oxidation of higher hydrocarbons. Therefore, their competition with the branching path exists even when different fuels are concerned, and in principle might cause oscillating dynamics also in such cases. To the authors' knowledge, no experimental data are available in very dilute conditions for heavier hydrocarbons to understand this. Nevertheless, a predictive numerical study is still possible, and the C_0-C_3 kinetic model introduced in Section 2.2 can be used to predict the establishment of limit cycles.

For the purposes of this work, the oxidation of ethylene is considered as case study. Using the same experimental conditions adopted for the combustion of CH_4 and described in Section 2.1, limit cycles were observed even in this case. The frequency map for stoichiometric mixtures, created with the non-isothermal model, is shown in Figure 13. Compared to Figure 5a, oscillations are predicted at lower temperatures, with both upper and lower limits ~100 K lower than the case with CH_4. The higher reactivity of C_2H_4 with respect to CH_4 explains this shift. In quantitative terms, the predicted frequency in the oscillating region is generally higher for C_2H_4 by one order of magnitude.

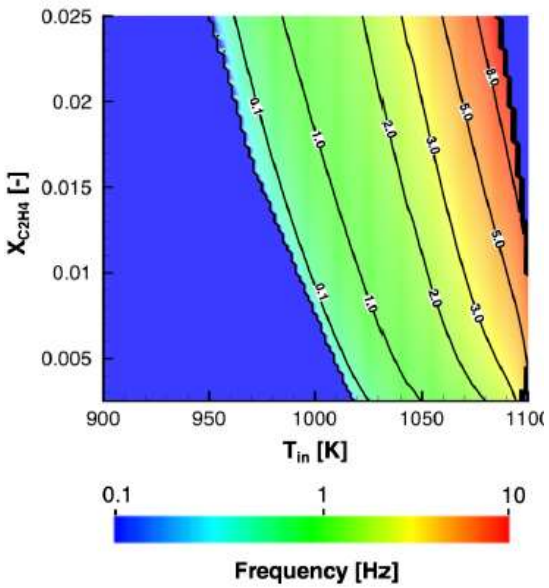

Figure 13. Predicted frequency of oscillations in the oxidation of C_2H_4 in a JSR, as a function of inlet temperature and fuel mole fraction (φ = 1, P = 107 kPa, τ = 2 s). Colorscale is logarithmic.

The time evolution of the major species following C_2H_4 oxidation is shown in Figure 14. Compared to CH_4 in similar conditions (Figure 8a), some important differences must be highlighted: first of all, fuel consumption is more gradual throughout the single cycle, such that C_2H_4 profile exhibits a right tail. This is due to its higher reactivity with respect to CH_4, such that it is almost immediately converted into the smaller radicals. As a result, CH_3 starts accumulating straight after extinction (like CH_3OH and HO_2), and its profile is bell-shaped rather than cusp-shaped (as it was instead in CH_4 oxidation). As expected, OH and H follow the same trends in the two cases, since their explosion is governed by the branching reaction. Figure 15 shows the bifurcation diagram in these conditions. The result that would be obtained if recombination reactions (1)–(5) were eliminated, is shown as well. In this case, the presence of termination reactions does

not result in steady-state multiplicity, i.e. ignition/extinction behavior. Anyway, two HBs are observed at approximately 1020 K and 1100 K, and 1000 K and 1100 K for an $X_{C_2H_4}$ equal to 0.0025 and 0.01, respectively. As no stable attractor is available in the temperature range between the two HBs, sustained oscillations are observed. When termination reactions are eliminated, steady state multiplicity exists with one HB on the ignited branch at a lower temperature than the ignition temperature, and another HB very close to the ignition point. In this case, oscillations would not be sustained, since the system would be attracted by the stable ignited or non-ignited state. This again shows the important role of the recombination reactions on the oscillatory behavior.

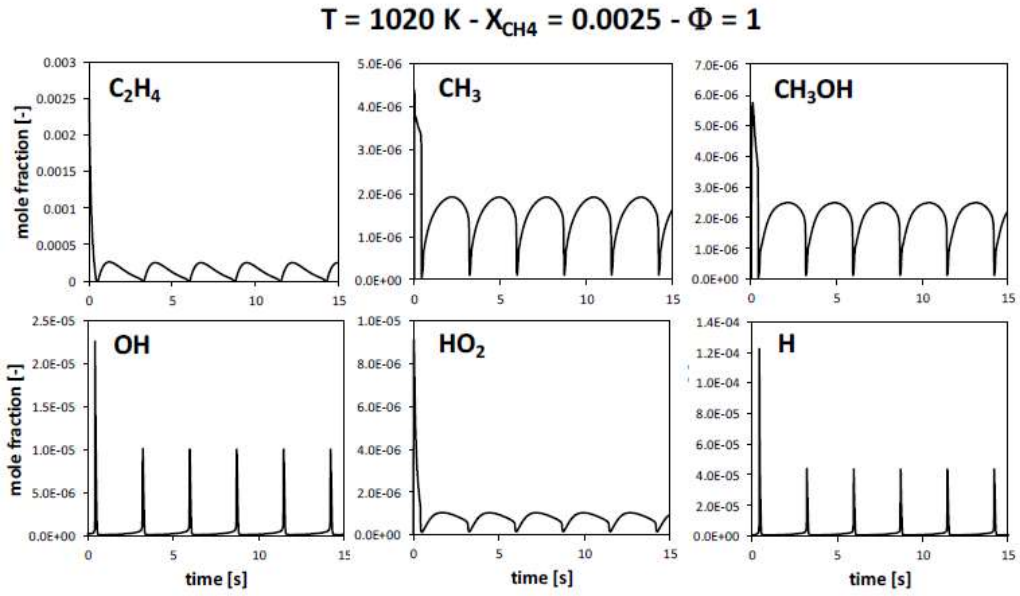

Figure 14. Predicted time profiles of representative species in the oxidation of ethylene in a JSR in very diluted conditions (P = 107 kPa, τ = 2 s).

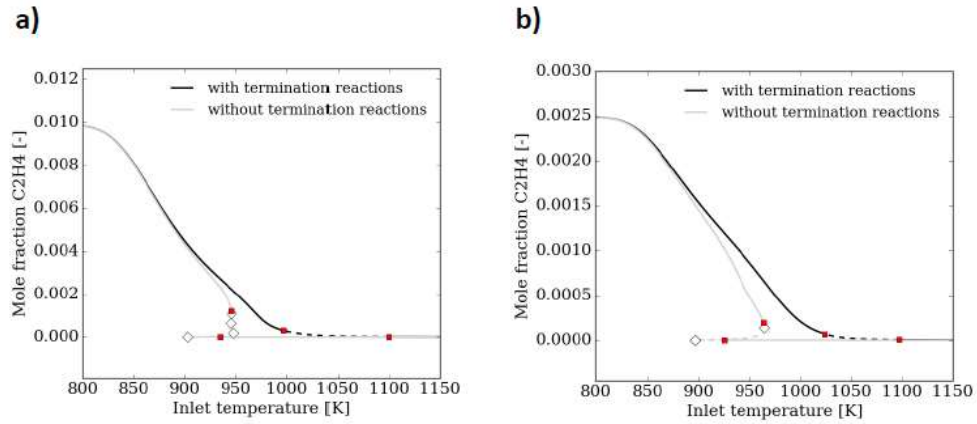

Figure 15. Influence of termination reactions on oscillation behavior during ethylene oxidation. P = 107 kPa, τ = 2 s. (a) φ = 1, $X_{C_2H_4}$ = 0.01. (b) φ = 1, $X_{C_2H_4}$ = 0.0025.

3.4. Coupling with heat exchange: propane oxidation in JSR

In less dilute conditions, thermal effects due to the interaction between heat release and heat loss play a major role, to the point that they must be taken into account for a comprehensive understanding of the oscillating behavior. This has been deeply investigated for CH_4 combustion [11,26-28,35], while for heavier hydrocarbons literature is much more limited. Recently, experimental data were obtained by Lubrano Lavadera et al. [33,34] for propane combustion with different diluents, with a mole fraction of diluent equal

to 90% (cfr. Table 1). In order to highlight the thermokinetic coupling and its effects on the onset of oscillations, the oxidation of propane in a JSR, in a bath of nitrogen, was studied by using C_0-C_3 kinetic model. Results are shown in Figure 16, where both isothermal and non-isothermal simulations were performed. For the latter, the suggested global heat exchange coefficient U = 54.4W/m/K was adopted. For these conditions, it can be observed that heat exchange affects conversion to a significant extent, while also determining the onset of oscillations. Reactivity is significantly underestimated with the isothermal model, while correctly predicted with the inclusion of heat exchange. In this latter case, the T range where oscillations occur is predicted quite well by the model, with a slight overestimation of the upper limit in stoichiometric conditions. Interestingly, with a leaner mixture the oscillating region is split into two parts, separated by an intermediate area where steady state is obtained. This can also be inferred from the experimental results, where for 1000 K $< T <$ 1100 K no clear distinction can be made between the regions characterized by steady-state and oscillating solutions, respectively.

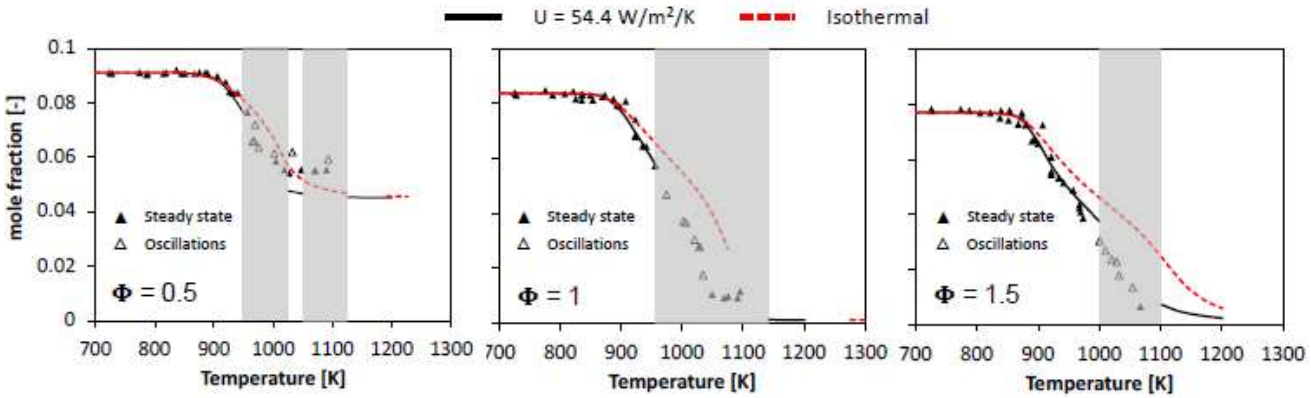

Figure 16. O_2 mole fraction following C3H8 oxidation in a JSR. Shaded area corresponds to oscillating solution, as predicted by the non-isothermal model. P = 1.1 atm, τ = 0.5 s, X_{N_2} = 0.9. Reactor geometries are defined in [34].

Bifurcation analysis of such predictions sheds further light on the thermokinetic interaction. As shown in Figure 17, the heat transfer coefficient has a controlling influence on the location of HBs, as well as on the temperature range where oscillations are established. In lean conditions, moving from the suggested value of U to higher values, the oscillation window at lower T disappears, while the second gradually shifts at higher temperatures. In the limiting case of perfect isothermality, one oscillating region remains at a higher temperature range. At rich conditions, increasing the heat transfer coefficient results in the progressive reduction of the oscillation range, up to its disappearance in isothermal conditions. Heat transfer also affects the shape of the bifurcation curve: apparently, lower values of U lead to steady-state multiplicity, which is a well-known consequence of the thermal backmixing in a CSTR.

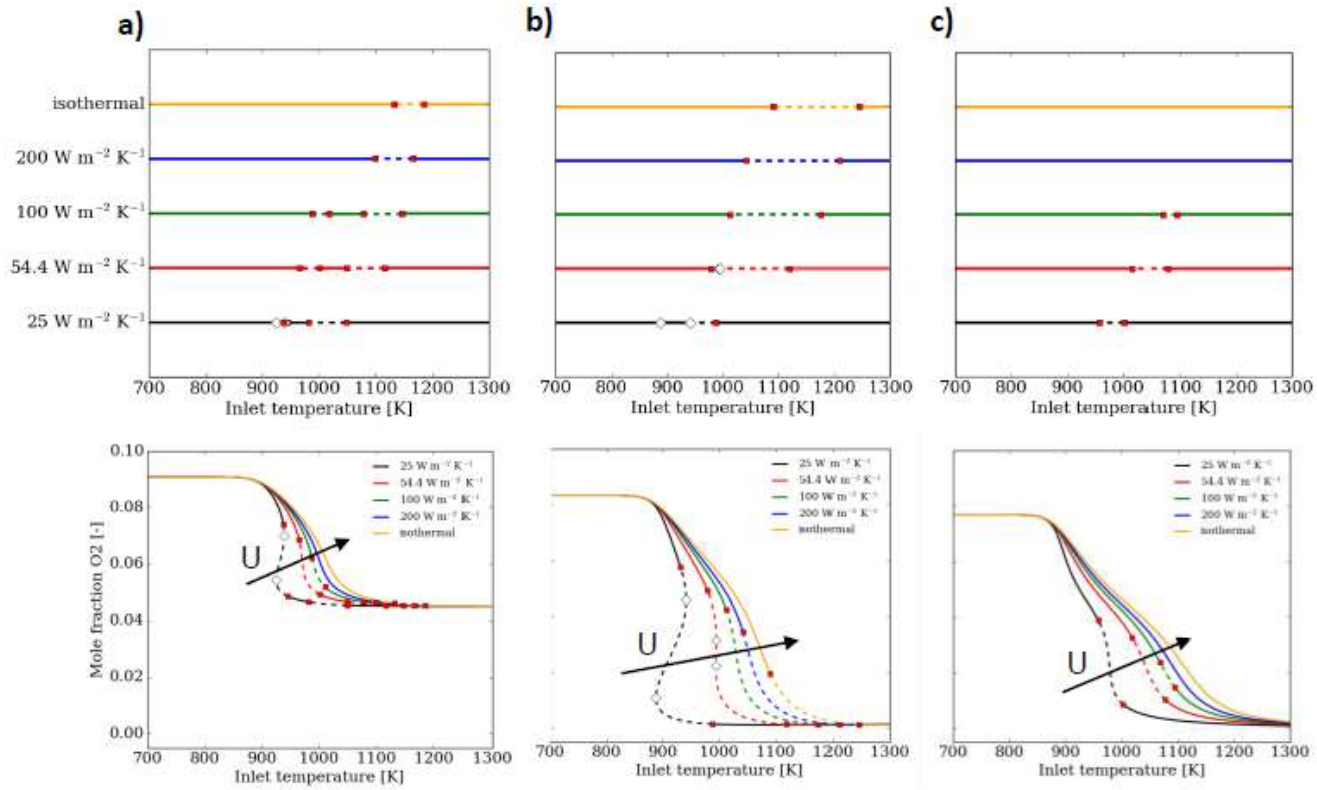

Figure 17. Influence of global heat transfer coefficient on oscillation behavior during propane oxidation. P = 1.1 atm, τ = 0.5 s. (a) φ = 0.5, $X_{C_3H_8}$ = 0.0091. (b) φ = 1, $X_{C_3H_8}$ = 0.0167. (c) φ = 1.5, $X_{C_3H_8}$ = 0.0231. N_2 used as bath gas (90% vol/vol).

4. Conclusions

The role of chemistry on oscillatory behaviors affecting hydrocarbons combustion was investigated under ideal conditions in a well-stirred system. The transient evolution of reactants and products mole fractions during the oscillating combustion of methane in a JSR were experimentally measured. In order to decouple chemical effects from heat exchange, very diluted mixtures were investigated such to obtain quasi-isothermal conditions, with fuel mole fractions between 0.25% and 2.5%. The combination of a fundamental kinetic model and bifurcation analysis allowed to identify the kinetic competitions that generate periodic limit cycles, valid for methane as well as higher hydrocarbons.

Frequency analysis also confirmed the reasonable accuracy of the kinetic model in predicting oscillation dynamics throughout the experimental operating range. The use of sensitivity analysis at the time instances before and after mixture ignition was crucial in identifying the inhibiting effect of 5 main recombination reactions after ignition, whilst fostering reactivity before ignition.

Bifurcation analysis showed that the decrease of the reaction rate of the recombination reactions progressively reduced the width of the oscillating region, up to the complete disappearance of the instabilities. The same behavior was predicted for heavier fuels, for which few experimental data are available. For ethylene combustion, similar trends were observed as for methane combustion, although no multiple states were observed in the presence of termination reactions.

The interaction between chemistry and heat exchange and its effects on the system stability was investigated with propane as fuel, for which experimental data have been recently collected. As opposed to the cases with methane as fuel, no multiplicity of steady states was observed, but only locally unstable

regions, with multiple Hopf Bifurcations giving rise to intermediate stable regions. The observed experimental overlap between steady-state and oscillating solutions confirmed such predictions. The bifurcation analysis and the comparison with isothermal simulations showed that this behavior is controlled by the competition between heat release and heat loss, in turn regulating the competition between branching and termination reactions.

Acknowledgements

This work has been carried out under the financial support of the IMPROOF project (H2020-IND-CE-2016–17/H2020-SPIRE-S016) within the European Union Horizon 2020 research and innovation program (grant agreement No. 723706). The authors would also like to acknowledge Fabio De Capitani (Politecnico di Milano) for the useful discussions. LAV also acknowledges financial support from a doctoral fellowship from the Fund for Scientific Research Flanders (FWO).

Supplementary material

- A word file with supplementary figures and tables.
- Three text files (reactions, thermodynamic properties and transport data) for the model under Chemkin format.

References

[1] The European Parliament and the Council of the European Union, Directive 2010/75/eu of the european parliament and of the council, Off. J. Eur. Union L 334 (2010) 17–119.

[2] S. Gan, H. K. Ng, K. M. Pang, Homogeneous charge compression ignition (hcci) combustion: implementation and effects on pollutants in direct injection diesel engines, Applied Energy 88 (3) (2011) 559–567.

[3] J. Chang, G. Kalghatgi, A. Amer, Y. Viollet, Enabling high efficiency direct injection engine with naphtha fuel through partially premixed charge compression ignition combustion, Tech. rep., SAE Technical Paper (2012).

[4] A. K. Agarwal, A. P. Singh, R. K. Maurya, Evolution, challenges and path forward for low temperature combustion engines, Progress in Energy and Combustion Science 61 (2017) 1–56.

[5] J. Wünning, J. Wünning, Flameless oxidation to reduce thermal no-formation, Progress in energy and combustion science 23 (1) (1997) 81–94.

[6] A. Cavaliere, M. de Joannon, Mild combustion, Progress in Energy and Combustion science 30 (4) (2004) 329–366.

[7] R. Hilbert, F. Tap, H. El-Rabii, D. Thévenin, Impact of detailed chemistry and transport models on turbulent combustion simulations, Progress in Energy and combustion science 30 (1) (2004) 61–117.

[8] J. Griffiths, S. Scott, Thermokinetic interactions: Fundamentals of spontaneous ignition and cool flames, Progress in energy and combustion science 13 (3) (1987) 161–197.

[9] C. K. Law, P. Zhao, Ntc-affected ignition in nonpremixed counterflow, Combustion and Flame 159 (3) (2012) 1044–1054.

[10] A. Stagni, D. Brignoli, M. Cinquanta, A. Cuoci, A. Frassoldati, E. Ranzi, T. Faravelli, The influence of low-temperature chemistry on partially-premixed counterflow n-heptane/air flames, Combustion and Flame 188 (2018) 440–452.

[11] M. De Joannon, P. Sabia, A. Tregrossi, A. Cavaliere, Dynamic behavior of methane oxidation in premixed flow reactor, Combustion science and technology 176 (5-6) (2004) 769–783.

[12] S. Sarsani, D. West, W. Liang, V. Balakotaiah, Autothermal oxidative coupling of methane with ambient feed temperature, Chemical Engineering Journal 328 (2017) 484–496.

[13] L. A. Vandewalle, I. Lengyel, D. H. West, K. M. Van Geem, G. B. Marin, Catalyst ignition and extinction: A microkinetics-based bifurcation study of adiabatic reactors for oxidative coupling of methane, Chemical Engineering Science.

[14] R. Aris, Chemical reactors and some bifurcation phenomena, Annals of the New York Academy of Sciences 316 (1) (1979) 314–331.

[15] P. Gray, J. Griffiths, S. K. Scott, Branched-chain reactions in open systems: theory of the oscillatory ignition limit for the hydrogen+ oxygen reaction in a continuous-flow stirred-tank reactor, Proc. R. Soc. Lond. A 394 (1807) (1984) 243–258.

[16] P. Gray, J. Griffiths, S. Scott, Oscillations, glow and ignition in carbon monoxide oxidation in an open system. i. experimental studies of the ignition diagram and the effects of added hydrogen, Proc. R. Soc. Lond. A 397 (1812) (1985) 21–44.

[17] D. Baulch, J. Griffiths, A. J. Pappin, A. F. Sykes, Stationary-state and oscillatory combustion of hydrogen in a well-stirred flow reactor, Combustion and flame 73 (2) (1988) 163–185.

[18] D. L. Baulch, J. F. Griffiths, A. J. Pappin, A. F. Sykes, Third-body interactions in the oscillatory oxidation of hydrogen in a well stirred flow reactor, Journal of the Chemical Society, Faraday Transactions 1: Physical Chemistry in Condensed Phases 84 (5) (1988) 1575–1586.

[19] D. Baulch, J. Griffiths, B. Johnson, R. Richter, Hydroxyl radical concentrations and reactant temperature profiles during oscillatory ignition of hydrogen: experimental measurements by laser resonance absorption spectroscopy and comparisons with numerical calculations, Proc. R. Soc. Lond. A 430 (1878) (1990) 151–166.

[20] B. R. Johnson, S. K. Scott, A. S. Tomlin, Modelling complex oscillations for the H_2+ O_2 reaction in an open system, Journal of the Chemical Society, Faraday Transactions 87 (16) (1991) 2539–2548.

[21] A. S. Tomlin, M. J. Pilling, T. Turányi, J. H. Merkin, J. Brindley, Mechanism reduction for the oscillatory oxidation of hydrogen: sensitivity and quasi-steady-state analyses, Combustion and flame 91 (2) (1992) 107–130.

[22] R. Brad, A. Tomlin, M. Fairweather, J. Griffiths, The application of chemical reduction methods to a combustion system exhibiting complex dynamics, Proceedings of the Combustion Institute 31 (1) (2007) 455–463.

[23] P. Gray, S. K. Scott, Chemical oscillations and instabilities: non-linear chemical kinetics, Vol. 21, Oxford University Press, 1994.

[24] K. Chinnick, C. Gibson, J. Griffiths, W. Kordylewski, Isothermal interpretations of oscillatory ignition during hydrogen oxidation in an open system. i. analytical predictions and experimental measurements of periodicity, Proc. R. Soc. Lond. A 405 (1828) (1986) 117–128.

[25] P. J. Ashman, B. S. Haynes, Rate coefficient of H + O_2 + M = HO_2 + M (M= H_2O, N_2, Ar, CO_2), in: Symposium (International) on Combustion, Vol. 27, Elsevier, 1998, pp. 185–191.

[26] M. De Joannon, A. Cavaliere, T. Faravelli, E. Ranzi, P. Sabia, A. Tregrossi, Analysis of process parameters for steady operations in methane mild combustion technology, Proceedings of the Combustion Institute 30 (2) (2005) 2605–2612.

[27] P. Sabia, M. De Joannon, S. Fierro, A. Tregrossi, A. Cavaliere, Hydrogen-enriched methane mild combustion in a well stirred reactor, Experimental Thermal and Fluid Science 31 (5) (2007) 469–475.

[28] P. Sabia, M. de Joannon, A. Picarelli, R. Ragucci, Methane auto-ignition delay times and oxidation regimes in mild combustion at atmospheric pressure, Combustion and Flame 160 (1) (2013) 47–55.

[29] M. Lubrano Lavadera, Y. Song, P. Sabia, O. Herbinet, M. Pelucchi, A. Stagni, T. Faravelli, F. Battin-Leclerc, M. d. Joannon, Oscillatory behavior in methane combustion: on the influence of the operating parameters, Energy & Fuels.

[30] G. Bagheri, M. L. Lavadera, E. Ranzi, M. Pelucchi, P. Sabia, M. de Joannon, A. Parente, T. Faravelli, Thermochemical oscillation of methane mild combustion diluted with N_2/CO_2/H_2O, Combustion Science and Technology 191 (1) (2019) 68–80.

[31] Y. Song, L. Marrodán, N. Vin, O. Herbinet, E. Assaf, C. Fittschen, A. Stagni, T. Faravelli, M. Alzueta, F. Battin-Leclerc, The sensitizing effects of NO_2 and NO on methane low temperature oxidation in a jet stirred reactor, Proceedings of the Combustion Institute 37 (1) (2019) 667–675.

[32] P. Gray, J. Griffiths, S. Hasko, Ignitions, extinctions and thermokinetic oscillations accompanying ;the oxidation of ethane in an open system (continuously stirred tank reactor), Proc. R. Soc. Lond. A 396 (1811) (1984) 227–255.

[33] M. L. Lavadera, P. Sabia, G. Sorrentino, R. Ragucci, M. de Joannon, Experimental study of the effect of CO_2 on propane oxidation in a jet stirred flow reactor, Fuel 184 (2016) 876–888.

[34] M. Lubrano Lavadera, P. Sabia, M. de Joannon, A. Cavaliere, R. Ragucci, Propane oxidation in a jet stirred flow reactor. the effect of h2o as diluent species, Experimental Thermal and Fluid Science 95 (2018) 35–43.

[35] P. Sabia, G. Sorrentino, A. Chinnici, A. Cavaliere, R. Ragucci, Dynamic behaviors in methane mild and oxy-fuel combustion. Chemical effect of CO_2, Energy & Fuels 29 (3) (2015) 1978–1986.

[36] P. Dagaut, M. Cathonnet, J. Rouan, R. Foulatier, A. Quilgars, J. Boettner, F. Gaillard, H. James, A jet-stirred reactor for kinetic studies of homogeneous gas-phase reactions at pressures up to ten atmospheres (_ 1 mpa), Journal of Physics E: Scientific Instruments 19 (3) (1986) 207.

[37] O. Herbinet, P.-M. Marquaire, F. Battin-Leclerc, R. Fournet, Thermal decomposition of n-dodecane: Experiments and kinetic modeling, Journal of analytical and applied pyrolysis 78 (2) (2007) 419–429.

[38] D. Matras, J. Villermaux, Un réacteur continu parfaitement agité par jets gazeux pour l'étude cinétique de réactions chimiques rapides, Chemical Engineering Science 28 (1) (1973) 129–137.

[39] O. Herbinet, G. Dayma, Jet-stirred reactors, in: Cleaner combustion, Springer, 2013, pp. 183–210.

[40] F. Battin-Leclerc, J. M. Simmie, E. Blurock, Cleaner combustion, Springer, 2013.

[41] P. J. Linstrom, W. Mallard, Nist chemistry webbook; nist standard reference database no. 69.

[42] E. Ranzi, A. Sogaro, P. Gaffuri, G. Pennati, T. Faravelli, A wide range modeling study of methane oxidation, Combustion science and technology 96 (4-6) (1994) 279–325.

[43] E. Ranzi, M. Dente, T. Faravelli, G. Pennati, Prediction of kinetic parameters for hydrogen abstraction reactions, Combustion science and technology 95 (1-6) (1993) 1–50.

[44] W. K. Metcalfe, S. M. Burke, S. S. Ahmed, H. J. Curran, A hierarchical and comparative kinetic modeling study of C_1- C_2 hydrocarbon and oxygenated fuels, International Journal of Chemical Kinetics 45 (10) (2013) 638–675.

[45] S. M. Burke, U. Burke, R. Mc Donagh, O. Mathieu, I. Osorio, C. Keesee, A. Morones, E. L. Petersen, W. Wang, T. A. DeVerter, et al., An experimental and modeling study of propene oxidation. Part 2: Ignition delay time and flame speed measurements, Combustion and Flame 162 (2) (2015) 296–314.

[46] A. Burcat, B. Ruscic, et al., Third millenium ideal gas and condensed phase thermochemical database for combustion (with update from active thermochemical tables)., Tech. rep., Argonne National Lab.(ANL), Argonne, IL (United States) (2005).

[47] A. Stagni, A. Frassoldati, A. Cuoci, T. Faravelli, E. Ranzi, Skeletal mechanism reduction through species-targeted sensitivity analysis, Combustion and Flame 163 (2016) 382–393.

[48] P. Pepiot-Desjardins, H. Pitsch, An efficient error-propagation-based reduction method for large chemical kinetic mechanisms, Combustion and Flame 154 (1-2) (2008) 67–81.

[49] K. E. Niemeyer, C.-J. Sung, M. P. Raju, Skeletal mechanism generation for surrogate fuels using directed relation graph with error propagation and sensitivity analysis, Combustion and flame 157 (9) (2010) 1760–1770.

[50] P. Dirrenberger, H. Le Gall, R. Bounaceur, P.-A. Glaude, F. Battin-Leclerc, Measurements of laminar burning velocities above atmospheric pressure using the heat flux method–application to the case of n-pentane, Energy & Fuels 29 (1) (2015) 398–404.

[51] E. Ranzi, A. Frassoldati, R. Grana, A. Cuoci, T. Faravelli, A. Kelley, C. Law, Hierarchical and comparative kinetic modeling of laminar flame speeds of hydrocarbon and oxygenated fuels, Progress in Energy and Combustion Science 38 (4) (2012) 468–501.

[52] T. Le Cong, P. Dagaut, G. Dayma, Oxidation of natural gas, natural gas/syngas mixtures, and effect of burnt gas recirculation: Experimental and detailed kinetic modeling, Journal of Engineering for Gas Turbines and Power 130 (4) (2008) 041502.

[53] M. Marek, I. Schreiber, Chaotic behaviour of deterministic dissipative systems, Vol. 1, Cambridge University Press, 1995.

[54] R. Seydel, Practical bifurcation and stability analysis, Vol. 5, Springer Science & Business Media, 2009.

[55] S. Subramanian, V. Balakotaiah, Classification of steady-state and dynamic behavior of distributed reactor models, Chemical Engineering Science 51 (3) (1996) 401–421.

[56] V. Balakotaiah, D. Luss, Multiplicity features of reacting systems: dependence of the steady-states of a CSTR on the residence time, Chemical Engineering Science 38 (10) (1983) 1709–1721.

[57] I. Lengyel, D. H. West, Numerical bifurcation analysis of large-scale detailed kinetics mechanisms, Current Opinion in Chemical Engineering 21 (2018) 41–47.

[58] S. Kalamatianos, D. Vlachos, Bifurcation behavior of premixed hydrogen/air mixtures in a continuous stirred tank reactor, Combustion science and technology 109 (1-6) (1995) 347–371.

[59] R. Shan, T. Lu, Ignition and extinction in perfectly stirred reactors with detailed chemistry, Combustion and Flame 159 (6) (2012) 2069–2076.

[60] L. Acampora, F. S. Marra, Numerical strategies for the bifurcation analysis of perfectly stirred reactors with detailed combustion mechanisms, Computers & Chemical Engineering 82 (2015) 273–282.

[61] M. Kooshkbaghi, C. E. Frouzakis, K. Boulouchos, I. V. Karlin, n-heptane/air combustion in perfectly stirred reactors: Dynamics, bifurcations and dominant reactions at critical conditions, Combustion and Flame 162 (9) (2015) 3166–3179.

[62] E. J. Doedel, T. F. Fairgrieve, B. Sandstede, A. R. Champneys, Y. A. Kuznetsov, X. Wang, Auto-07p: Continuation and bifurcation software for ordinary differential equations.

[63] D. G. Goodwin, H. K. Moffat, R. L. Speth, Cantera: An object-oriented software toolkit for chemical kinetics, thermodynamics, and transport processes, Caltech, Pasadena, CA.

[64] S. A. Fulop, K. Fitz, Algorithms for computing the time-corrected instantaneous frequency (reassigned) spectrogram, with applications, The Journal of the Acoustical Society of America 119 (1) (2006) 360–371.

[65] G. P. Smith, D. M. Golden, M. Frenklach, N. W. Moriarty, B. Eiteneer, M. Goldenberg, C. T. Bowman, R. K. Hanson, S. Song, W. Gardiner Jr, et al., Gri-mech 3.0, URL http://www. me.berkeley. edu/gri_mech.

[66] B. Wang, H. Hou, L. M. Yoder, J. T. Muckerman, C. Fockenberg, Experimental and theoretical investigations on the methyl- methyl recombination reaction, The Journal of Physical Chemistry A 107 (51) (2003) 11414–11426.

[67] R. Fernandes, K. Luther, J. Troe, V. Ushakov, Experimental and modelling study of the recombination reaction $H+O_2(+M)=HO_2(+M)$ between 300 and 900 k, 1.5 and 950 bar, and in the bath gases M = He, Ar, and N_2, Physical Chemistry Chemical Physics 10 (29) (2008) 4313–4321.

[68] A. W. Jasper, S. J. Klippenstein, L. B. Harding, B. Ruscic, Kinetics of the reaction of methyl radical with hydroxyl radical and methanol decomposition, The Journal of Physical Chemistry A 111 (19) (2007) 3932–3950.

[69] J. Li, Z. Zhao, A. Kazakov, F. L. Dryer, An updated comprehensive kinetic model of hydrogen combustion, International journal of chemical kinetics 36 (10) (2004) 566–575.